

# Emergent helicity in free-standing semiflexible, charged polymers

Debarshi Mitra and Apratim Chatterji\*  
*Dept. of Physics, IISER-Pune, India-411008.*  
(Dated: April 13, 2023)

Helical motifs are ubiquitous in macromolecular systems. The mechanism of spontaneous emergence of helicity is unknown, especially in cases where torsional interactions are absent. Emergence of helical order needs coordinated organization over long distances in polymeric macromolecules. We establish a very generic mechanism to obtain spontaneous helicity by inducing screened Coulomb interactions between monomers in a semiflexible heteropolymer. Due to changes in solvent conditions, different segments (monomers) of a polymeric chain can get locally charged with charges of differing polarities and magnitudes along the chain contour. This in turn leads to spontaneous emergence of transient helical structures along the chain contour for a wide range of Debye-lengths. We have avoided using torsional potentials to obtain helical structures and rely only on radially symmetric interactions. Lastly, transient helices can be made long-lived when they are subjected to geometric confinement, which can emerge in experimental realizations through a variety of conditions.

## I. INTRODUCTION

The helical motif is a recurrent feature of several macro-molecular systems and is found in disparate systems in nature. These systems may be as varied as the chromosome of bacterial cells [1] and the secondary structure of proteins or actin filaments or in collagen molecules [2–5]. Thus, the helical structure is ubiquitous in the macro-molecular world. This has spurred a number of studies that investigate their emergence in several natural systems [4, 6–15]. Furthermore, helical motifs in synthetic molecules have been explored for their key technological ramifications [16] such as the synthesis of NEMs devices [17–22], piezoelectric devices [23] and other optical materials [24–26]. For these applications, helical molecules are typically designed using techniques such as vapour deposition which rely on specific interactions between the constituent monomers. Alternatively, helical templates are also often employed [27–32].

It would be of interest to unearth mechanisms by which one may induce chains to spontaneously self-organize to obtain helical structures at the  $nm$  to  $\mu m$  length scales. If these mechanisms are generic in nature and independent of the chemical details of the monomers, then one can have an alternative strategy of designing synthetic helical macro-molecules in the laboratory. More significantly, such studies would also shed light on the mechanisms governing the formation of helical structures in nature, both inside and outside the living cell.

Previous reports have demonstrated the formation of extremely short-lived helical polymers in bad solvents undergoing collapse [8]. The packing of tubular filaments in confined cylinders also lead to helix formation for particular ratios of pitch and radius [6]. Yet, another study shows that the ground state of a self-attracting chain shows a variety of structural motifs including the helix, depending on the nature of the stiffness present in

the chain (energetic or entropic) [11, 33]. In our previous work we showed that a bead-spring model of a semiflexible polymer chain with monomers all having the same value and polarity of charges and long range Coulomb interaction between monomers attains a transient helical conformation, when repulsive interactions are switched on between the monomers [34]. The monomers may become charged because of a change in the nature of the solvent, or if the ionic concentration of the solvent is suddenly changed or due to other changes in its environment. We obtained transient helices even when we replaced Coulomb interactions by long range repulsive power-law interactions.

Here we introduce a more generic model and establish that a semiflexible polymer chain with charged beads, each carrying a different value of charge and polarity, can also attain a transient helical conformation even due to the short range screened (spherically symmetric) Coulomb interactions between the monomers. This scenario is likely to occur in many natural systems. Additionally, we show that asymmetry in the distribution of charges along the polymer chain plays a pivotal role in helix formation. A chain with an approximately equal number of positive and negative charges does not form helices. The helix formation takes place only for a certain range of parameters of the polymer, such as the persistence length, the spring constant, the Debye length etc. We further show that the helices formed by these screened electrostatic interactions can be made long-lived under geometric confinement, in a cuboid of appropriate dimensions.

In the case of bacterial nucleoids, this geometric confinement can be imposed by the bacterial cell leading to stable helical structures of nucleoids. These beads can be molecular units of a heteropolymer, or groups of amino acid sequences with length scale of the size of the beads, or even larger units of molecules such as nucleosome complex in the DNA dressed by suitable (charged) proteins, or even polymeric chains where the monomeric units are micron sized colloids. In this case, the colloidal surface can be dressed by microgel particles which have

---

\* Correspondence email address: apratim@iiserpune.ac.in

been cross-linked together as shown by [14, 35]. The colloidal particles then form a polymeric chain held together by cross-links with tunable semiflexibility (persistence length). If one uses colloids that are chemically different to each other, to form the chain, a change in the ionic concentration in the solution can result in a different value of charge on each colloid.

## II. MODEL

We use Brownian dynamics simulations to study helix formation in a single semiflexible, bead-spring model of a polymer chain, where the monomers have different values of charges along the chain contour as determined by a probability distribution. The center of each monomer is connected by harmonic springs of spring constant  $\kappa$  and of equilibrium length  $a$  to the center of two neighbouring monomers. We choose  $a$  to be the unit of length for our simulations. Furthermore, there is a bending energy cost per every triplet of monomers along the chain contour to incorporate effects of semiflexibility. The energy cost of having bends along the chain, is realized by the bending potential  $V(\theta) = \epsilon_B \cos(\theta)$ , where  $\theta$  is the angle between the bond vectors  $(-\mathbf{r}_i, \mathbf{r}_{i+1})$ . The vector  $\mathbf{r}_i$  is the vector joining monomer  $i - 1$  to its neighbouring monomer  $i$  along the chain contour. The quantity  $\epsilon_B$  can also be directly related to the persistence length  $\ell_p$ ,

$$\ell_p \approx a\epsilon_B/k_B T \quad (1)$$

for small deviations of  $\theta$  from  $\pi$ , refer appendix of [34]. In our simulations, energy is measured in units of the thermal energy  $k_B T$ . The excluded volume of the monomers are modelled by the WCA (Weeks, Chandler, Andersen) potential and all the monomers have diameters  $\sigma = 0.7a$ .

Additionally, any two monomers  $i$  and  $j$  situated at a distance  $r_{ij}$  from each other, with charges  $q_i$  and  $q_j$  interact with each other through the screened Coulomb interaction.

$$V(r_{ij}) = \frac{q_i q_j}{4\pi\epsilon r_{ij}} \times \exp(-r_{ij}/\lambda_D) \dots \forall r_{ij} < r_c \quad (2)$$

where the Debye length  $\lambda_D$  is a parameter and sets the length scale over which Coulomb interactions get screened out. The permittivity  $\epsilon$  of the background medium within which the chain is suspended, can be expressed in terms of the permittivity of vacuum  $\epsilon_0$  and the relative permittivity  $\epsilon_r$ . The strength of interactions is determined by the value of  $q_i$  and  $q_j$ , but for our calculation we will express charge in units of  $Z_0$ , such that the interaction between any two charged monomers can be expressed as:

$$V(r_{ij}) = Z_i Z_j / r_{ij} \times \exp(-r_{ij}/\lambda_D) \dots \forall r_{ij} < r_c \quad (3)$$

where,  $Z_i$  and  $Z_j$  denote the value of charges and is expressed in units of  $Z_0$ , on the interacting monomers in

simulation units. In the subsequent section, we elaborate on how the values of  $Z$  can be related to charge in real units.

We assign charges to the monomers in the chain such that there is stochasticity in the distribution of charges along the polymer chain. The charge  $Z_i$  of each monomer  $i$  in simulations will be allocated in terms of the asymmetry parameter  $\psi$  and  $Z_0$  such that  $Z_i = Z_0 \times (r - \psi)$ , where  $r$  is a random number whose values are chosen from a uniform distribution of random numbers between 0 and 1. We vary  $\psi$  between 0 and 1 to estimate the net charge of the chain. A value of  $\psi = 1$  implies that all monomers have random values of charges between  $Z_1 = 0$  and  $Z_2 = -Z_0$  s.u. A value of  $\psi = 0$  implies that all monomers have random values of charges between  $Z_1 = 0$  and  $Z_2 = Z_0$  s.u. Correspondingly, for  $\psi = 0.5$ , the charge on the monomers can take random values between  $Z_1 = -Z_0/2$  to  $Z_2 = Z_0/2$  s.u. Thus, in general, the charge on a monomer  $i$  can vary between  $Z_1$  and  $Z_2$ .

We will establish later in the manuscript that if  $\psi = 0.5$  such that there are statistically equal number of positive and negative charges, then we do not obtain helices. We need to introduce asymmetry in the distribution of charges using  $\psi$ , such that  $Z_1 \neq Z_2$ . The degree of asymmetry in the distribution of charges along the polymer chain is denoted by the quantity  $\psi$ . Thus,  $\psi = 0.1$  corresponds to a chain that statistically has 90% of the monomers having a positive charge.

For our Brownian dynamics simulations where the friction constant is  $\zeta$ , and the unit of time  $\tau$  is set by  $\tau = a^2\zeta/k_B T$ , the time taken for an isolated monomer to diffuse a distance of  $a$ . If we set  $\zeta = 1$  such that  $\tau = 1$  with  $k_B T = 1$  and  $a = 1$  (units of energy and length, respectively), the over-damped stochastic Brownian dynamics equation is integrated with time step  $dt = 0.0001\tau$ .

### A. Relevance to experimental systems

We now establish a correspondence between the magnitudes of charges used in the simulation (expressed in s.u.), and the magnitudes of charges in real units. If two monomers having unit charges in the simulations, are at a unit distance away from each other then they interact with Coulomb potential energy of strength  $k_B T$ . Let  $q_o$  be the charge in real units, corresponding to  $Z = 1$  s.u., where  $Z$  denotes the charge on a monomer in the simulations.

In real units two charges ( $q_o$ ) of identical charges have potential energy given by

$$\frac{(q_o)^2}{4\pi\epsilon a} = \frac{Z^2}{a} = k_B T \quad (4)$$

Thus at room temperature of  $T = 300K$ , the value of  $q_o$  in water ( $\epsilon_r = 80$ ) placed at unit distance ( $a$ ) is given by,

$$q_o = \sqrt{4\pi\epsilon a k_B T} = \sqrt{37 \times 10^{-30} a} C. \quad (5)$$

where the charge  $q_o$  is measured in Coulomb (C). If we choose  $a = 1nm$ , then  $q_o = 1.9 \times 10^{-19}C$ , or  $1.2e$ , where  $e$  denotes the electronic charge. If  $a = 10nm$  then we obtain  $q_o \approx 4e$ . If  $a = 100nm$  then,  $q_o \approx 12e$  and if  $a = 1\mu m$  then  $q_o \approx 40e$ . In this study we often use  $Z_0 \sim 10s.u$  which corresponds to a charge of  $40e$  for a monomer with size 10 nm. But that is the maximum charge on a monomer for  $\psi = 1$ . For lower values of  $\psi$ , the maximum charge that a monomer can take will be lower. Thus, the charges used in this study may feasibly occur in many macro-molecular systems.

### III. RESULTS

#### A. Helix Formation

We observe spontaneous emergence of helices if a uncharged semiflexible polymeric chain acquired charges at time  $t = T_0$  due to change in external conditions, e.g. change in pH of the solvent in which it is immersed. The helices formed are transient but may be stabilized by other factors such as hydrogen bond and geometric confinement, as we show later. We establish that the stochasticity in the value or sign of the charges on the monomers along the chain contour do not affect helix formation as long as there is sufficient asymmetry (as determined by  $\psi$ ) in the charge distribution. We have tried out different initial conditions, such that monomers  $i-1, i, i+1, i+2$  have different value of charges in different runs for a particular value of  $\psi$  (refer to the Methods section for the definition of  $\psi$ ) and monitor the helicity developed as we switch on charges on the monomers.

We measure helicity using the order parameters  $H2$  which is defined as

$$H2 = \frac{1}{N-3} \left( \sum_{i=2}^{i=N-2} \mathbf{u}_i \cdot \mathbf{u}_{i+1} \right) \quad (6)$$

where  $\mathbf{u}_i$  is the unit vector of  $\mathbf{U}_i = \mathbf{r}_i \times \mathbf{r}_{i+1}$ . A simple uncharged, semi-flexible polymer chain shows  $H2$  values  $\approx 0$  (or negative values of  $H2$ ) as expected for a chain locally bent due to thermal fluctuations, while calculating  $H2$  over helical segments of a polymer chain would lead to high positive values of  $H2$  [14, 34].

Past studies [8, 34] have also used another order parameter which is given by,

$$H4 = \frac{1}{N-2} \left( \sum_{i=2}^{i=N-1} \mathbf{u}_i \right)^2; \quad (7)$$

A perfect helix with uniform handedness, will have vectors  $u_i$  pointing along the helix axis, and hence  $H4$  will

have a value of  $\approx 1$ . However, if one obtains a helical polymer where half of the chain is right-handed, and the rest of it is left-handed,  $H4$  will be zero. In this study, we do not have any control over the handedness of the helical structures and thus for long chains, the chain is likely to have an equal number of right-handed and left-handed segments. Thus, we use the parameter  $H2$  to quantify helicity, in the remainder of the manuscript. In the future, we will report how we can design left handed and right handed helices, made to order.

We start our simulations with a uncharged semiflexible polymer chain in a heat bath, allow the chain to reach equilibrium over  $t = T_0 = 10\tau$  ( $10^5$  iterations), and switch on charge on the monomers thereafter. We show the various stages of helix formation through representative snapshots give in Fig.1(a-c). We also show that the helical polymer chain can easily be distinguished from a non-helical, uncharged, semiflexible polymer chain using  $H2$ , which fluctuates near zero till  $t = 10\tau$  and then show a finite non-zero value. In Fig.1d we show  $H2$  as a function of time  $t$  for three independent runs. In Fig.1e, we plot the end to end distance  $R_{ee}$ , scaled by the contour length  $R_C$  ( $R_c = 99a$ ) as a function of time. We see that the end to end distances fluctuate at values  $\approx 1$  for three independent runs till  $t = 10\tau$ , and thereafter the  $R_{ee}/R_c$  shows a sudden increase. Thus we show that the helix formation is independent of the initial configuration of the monomers as well on the stochastic distribution of charges along the chain contour.

**Mechanism of helix formation:** The uncharged semiflexible polymer chain undergoes stochastic conformational fluctuations due to the thermal noise from  $t = 0$  to  $t = 10\tau$ . When the electrostatic interactions are switched on, electrostatic forces leads to a reinforcement of the angular conformations with larger deviations in the angle  $\theta$  from the chain axis. This is because neighbouring charges repel each other, and move neighbouring monomers along the line joining their centers, and away from the chain axis. These angular conformations (with large angular deviations) are penalised due to the semiflexibility. As the different chain segments along the chain contour locally *straighten and stretch* out from the axis to reduce bending energy costs, the polymer consequently attains a helical conformation.

This can be surmised from Fig.2 where we plot the different energy contributions in the system, for parameters identical to that of Fig.1. In Fig.2a we plot the energy per spring,  $U_H$  versus time  $t$ . We see that at  $t < T_0$ ,  $U_H$  fluctuates around  $0.5k_B T$ , as expected from the equipartition theorem. However at  $t = 10\tau$ , we see that  $U_H$  shows a drastic increase which indicates that the bonds get stretched severely as a consequence of the electrostatic (e.s) interactions. This is further corroborated by the data presented in Fig.2b where we plot the screened Coulomb energy per monomer  $U_{sc}$  as a function of time. We see that at  $t = 10\tau$ ,  $U_{sc}$  shows a sudden spike which subsequently relaxes to lower values.

We also look at the bending energy  $U_b$  per triplet of

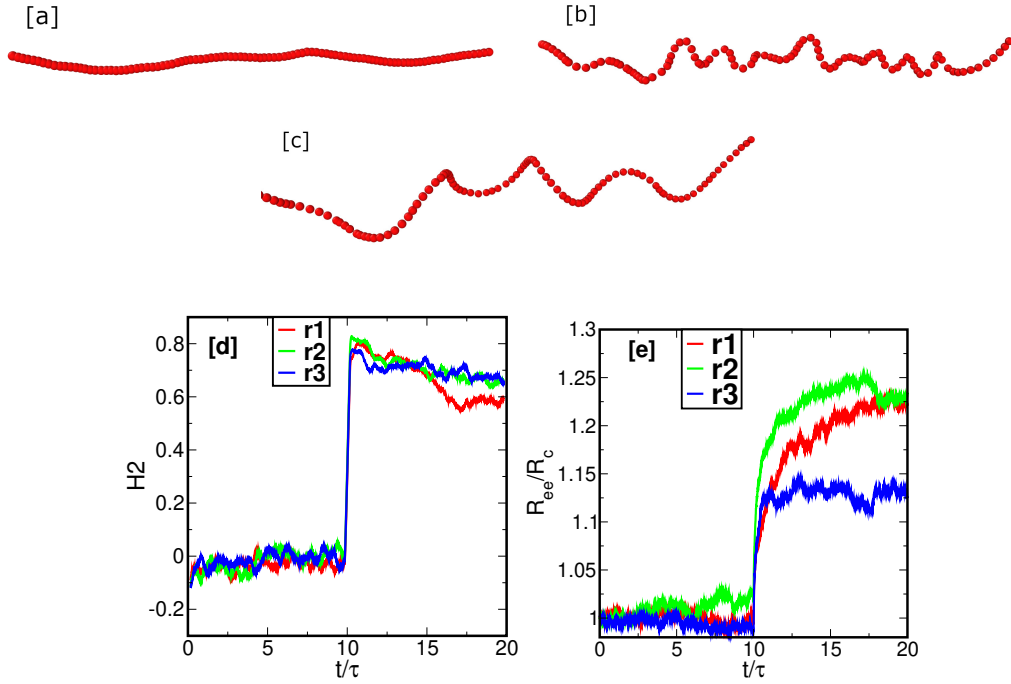


Figure 1. **Helix formation:** The snapshots shows various stages of the helix formation in a bead-spring model of a semi-flexible polymeric chain with 100 monomers, with contour length  $R_c = 99a$ . Initially, the uncharged polymer is in equilibrium with a thermal bath : representative snapshot shown in [a] at time  $t = 3\tau$ . Snapshot [b] shows a representative conformation of the chain soon after the monomers acquires charge at time  $t = 10\tau$ , where we see formation of helices along the chain contour. At (c)  $t = 20\tau$ , we see that the helix gradually “unwinds” and relaxes to a helical conformation having a larger pitch. The charge on each monomer has a random value, between  $-4.0$  to  $36$  s.u. (simulation unit). This corresponds to a asymmetry parameter of  $\psi = 0.1$  (refer to the Methods section for the definition of  $\psi$ ) and  $Z_0 = 40$  s.u. The bending energy cost  $\epsilon_B = 200k_B T$  (corresponding to a persistence length of  $200a$  and spring constant  $\kappa = 100k_B T/a^2$ , and the Debye length  $\lambda_d = 5a$ ). In (d) we show the helical order parameter  $H2$  (running averaged over  $0.33\tau$ ) as a function of simulation time  $t/\tau$ , for 3 independent runs. We see a sharp rise in  $H2$  at time  $t = 10\tau$ , which decays thereafter, indicating transient helix formation. Subfigure (e) shows the end to end distance  $R_{ee}/R_c$  versus  $t/\tau$ .

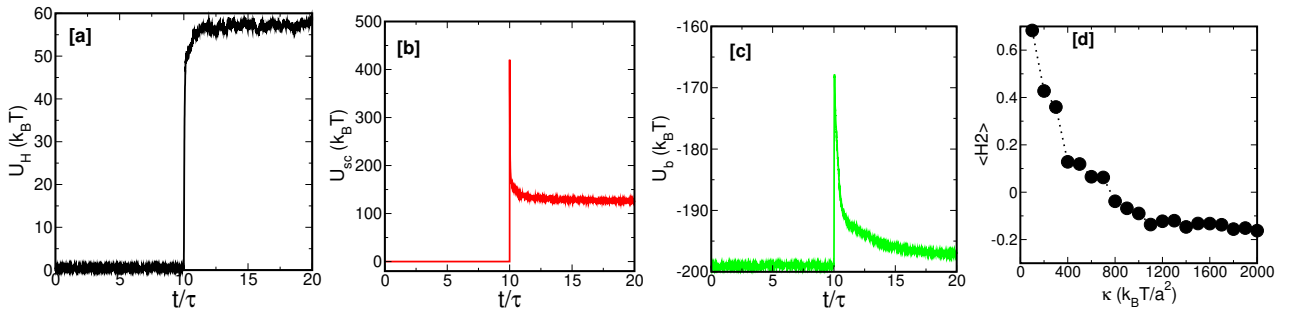


Figure 2. **Mechanism of Helix formation:** In (a), (b) and (c) we show the harmonic spring energy ( $U_H$ ), the screened coulomb energy ( $U_{sc}$ ) and the bending energy ( $U_b$ ) per monomer. We see that just after the screened Coulomb interaction is switched on, the screened coulomb energy and the bending energies peak, and subsequently relax leading to the “unwinding” of the helix. The springs in the polymer chains however continue to remain stretched due to the screened Coulomb interactions, as shown in (a). The sudden switching on of screened Coulomb interactions at  $t = 10\tau$ , leads to the formation of sharp angular conformations. This can be inferred by noting that  $U_b$  shows a peak at this point, in the plot given in (b). Subsequently, the transient helix formation takes place by the gradual relaxation of these sharp bends. Furthermore, if the springs are made too stiff, these sharp bends are not formed since a high value of  $\kappa$  prevents the monomer-bonds from stretching. Thus, in (d) we show that  $\langle H2 \rangle$  shows a monotonic decrease with increase in  $\kappa$ . We calculate the time averaged  $\langle H2 \rangle$  over  $10\tau$  to  $20\tau$ . The values of other parameters are same as that of the data presented in Fig.1.

monomers, in Fig.2c and we find that at  $t = T_0 = 10\tau$ , the bending energy shows a sudden spike, indicating a

sharply kinked (angular) conformation. However, such a conformation is penalised by the bending energy which prevents such sharp angles. Thus the helix formation occurs as a relaxation of transiently formed sharp angles. We emphasize again that the helix formed is transient and eventually the helical conformation dissolves. Thereafter, the polymer chain adopts an extended linear configuration due to the electrostatic interactions. Furthermore, thermal fluctuations play a pivotal role in the helix formation in creating the initial small bends which get accentuated after switching on the charge on the monomers. The transient helices do not form, if we switch on charge at temperature  $T = 0$ , as there are no thermal fluctuations. This has been explored in detail in [34], previously.

The importance of the formation of kinks in the subsequent emergence of helicity can also be gauged by the increasing the simulation  $\kappa$  parameter to high values, keeping  $k_B T = 1$ . We monitor the time averaged value of  $H2$  with increasing  $\kappa$  in Fig.2d, and observe that  $\langle H2 \rangle$  decreases with increasing  $\kappa$ . An increase in the spring constant prevents the bonds from stretching as much, and thereby formation of kinks on switching on of charges, and that in turn suppresses subsequent helix formation.

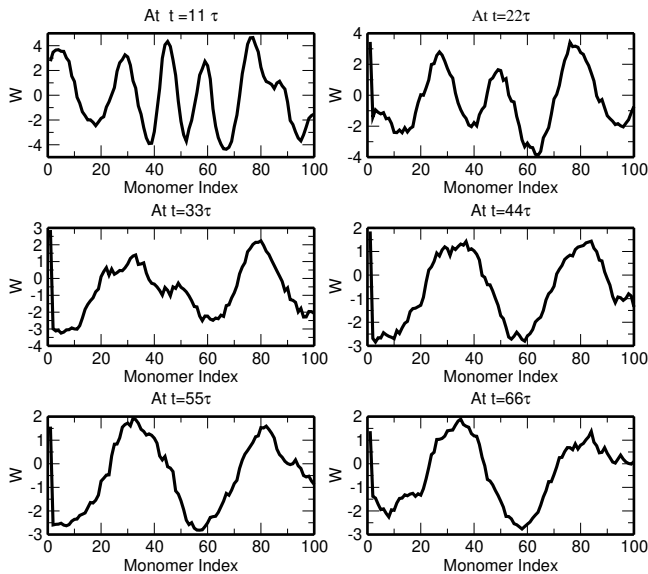


Figure 3. **Unwinding of the helix: Change in helical pitch** To quantitatively establish the unwinding of the helical polymer we look at the periodicity parameter  $W$  as a function of time.  $W$  is a scalar quantity resulting from the dot product of bond vectors along the chain contour with a vector perpendicular to the axis of the helical polymer chain. The periodicity in  $W$  indicates the pitch of the helix. In sub-figure (a) we show  $W$  for different times for a chain of 100 monomers, where we have switched on electrostatic interactions at  $t = 10\tau$ . The other parameters are also identical to that of the data presented in Fig.1 We note that due to the gradual unwinding of the helical polymer the periodicity in  $W$  decreases.

### Unwinding of the transient helices

The emergent structure of helices “unwind” with time. There are two factors that contribute to the unwinding: the bending energy and the screened coulomb interaction. The high energy cost of bending leads to the gradual relaxation of “kinks” (sharp angles) along the chain contour and thus leads to a straightening of the chain, such that  $\theta \approx \pi$ . This results in a gradual dissolution of the helical structures. The repulsive electrostatic interaction also leads to an “effective” additional bending energy cost [36] and causes the polymer chain to adopt an extended configuration. Thus the helix formation occurs only as a kinetic pathway to an extended linear equilibrium conformation.

To quantify this unwinding process, we look at the periodicity parameter  $W$  as a function of time.  $W$  is essentially the dot product of bond vectors along the contour with a vector perpendicular to the axis of the helical polymer chain. We initialize the chain along the  $\hat{y}$  direction. The helical axis of the emergent helix is also along  $\hat{y}$ . Thus, we calculate  $W$  as

$$W(i) = \hat{x} \cdot r_i \quad (8)$$

where  $r_i$  denotes the bond vectors along the chain contour, and  $i$  denotes the monomer indices along the chain contour. We now quantitatively establish that the helical conformations of the polymer relax by gradual unwinding. To that end we plot in Fig.3 the periodicity parameter  $W$  at various times, during the simulation run. We note that the periodicity in  $W$  decreases as simulation time elapses. This indicates that the helical polymer gradually unwinds and the pitch keeps on increasing. At any given time there may be helical segments of varying pitch, which gradually increase. Note that the most frequently occurring pitch of the helix along the chain contour, can be found from the data presented in Fig.3 by conducting a Fourier transform [34].

The most frequently occurring pitch of the helix  $P$  at a particular time also depends on the value of the bending energy  $\epsilon_B$ . A high value of  $\epsilon_B$  leads to larger values of  $P$  at a particular instant of simulation time. The other parameters do not affect the pitch of the helix.

### B. Parameters controlling helix formation

There are 4 system parameters which can be tuned to obtain the helical conformations in polymers. They are:

1. The magnitude of the charge on a monomer which is proportional to  $Z_0$ .
2. The Debye length of the screened Coulomb interaction:  $\lambda_D$ .
3. The bending energy  $\epsilon_B$ , which is directly proportional to the persistence length [34].
4. The degree of asymmetry in the charge distribution along the polymer chain.

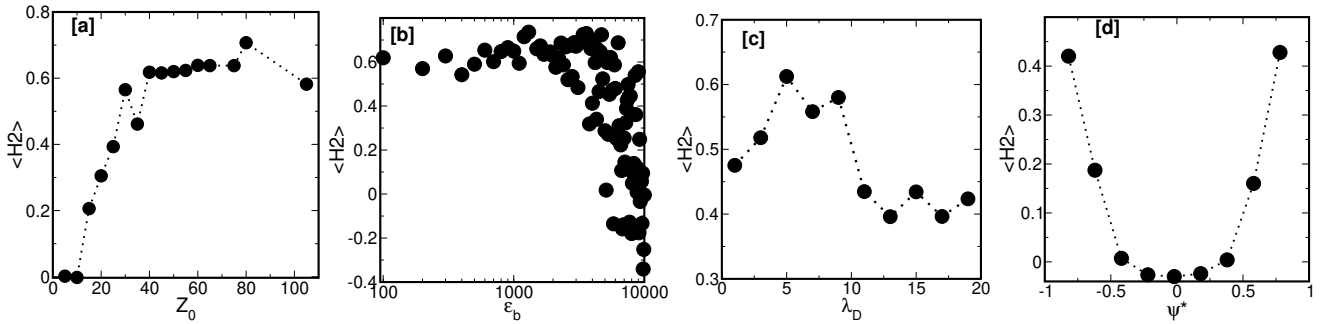


Figure 4. **Range of parameters conducive to helix formation:** For this set of subfigures (a-d), we keep the parameters  $Z_0$ ,  $\epsilon_B$ ,  $\lambda_D$ ,  $\kappa$ , and the asymmetry parameter  $\psi$  identical to that in Fig.1, but then vary one parameter at a time keeping the others fixed. We plot the time averaged helicity order parameter  $\langle H2 \rangle$  to analyze the helix formation as we modify different system parameters. Subfigure (d) shows the dependence of  $\langle H2 \rangle$  on the charge asymmetry parameter  $\psi^* = 1 - 2\psi$ . The quantity  $\psi^*$  indicates the asymmetry in the charge distribution in the polymer chain. The data in (c) and (d) has been produced by averaging over 10 independent runs.

In Fig.4, we investigate how helix formation depends on a balance of system parameters, and thereby plot the time averaged  $\langle H2 \rangle$  as we vary the parameters one at a time. Thereby, we keep the simulation parameters identical to those used to obtain data of Fig.1, and vary one parameter at a time. We compute the time averaged  $\langle H2 \rangle$  over a duration of  $10\tau$  from  $t = 10\tau$  to  $t = 20\tau$ .

In Fig.4a, we show that an increase in  $Z_0$ , i.e. maximum value and range of charges of the monomers along the chain, leads to an increase in helical order obtained. We observe an increase in  $\langle H2 \rangle$  with increase in  $Z_0$  before it plateaus around 0.6. Moreover, the quantity  $\langle H2 \rangle$  shows a decrease with increase in  $\epsilon_B$  as shown in Fig.4b. This is because an increase in the bending energy (or equivalently the persistence length  $\ell_p$ ) prevents the formation of sharp angular conformations as a response to the turning on of electrostatic forces. As mentioned before, the formation of sharp angular conformations (kinks) at time  $t = T_0$  are crucial to the subsequent formation of helices. Furthermore a higher chain rigidity also leads to the faster “unwinding” and dissolution of the transient helices.

An increase in the Debye length  $\lambda_D$  leads to a larger number of electrostatic interactions between monomers and thus leads to a greater propensity of helix formation. This leads to high values of  $\langle H2 \rangle$  for  $\lambda_D$  in the range of  $5 - 10a$ . Interestingly we see in Fig.4c that  $\langle H2 \rangle$  shows a non-monotonic dependence on  $\lambda_D$ . Note that here we have  $\psi = 0.1$  (or  $\psi^* = 0.8$ ) which implies that the majority of the charges along the chain have a positive value. When  $\lambda_D$  is increased then the strength of repulsive interactions increase leading to an increase in the helicity. However when  $\lambda_D$  is increased further then there are also attractive interactions along the chain (due to some monomers having charges of opposite polarity) that each monomer experiences. This leads to a decrease in the propensity for helix formation and consequently lower values for  $\langle H2 \rangle$  as there are strong attractions between different chain segments. This in turn suppresses

the effects of bending energy costs which led to helix formation. We discuss the consequence of increasing  $\lambda_D$  for a lower value of  $\psi$  subsequently. We emphasize that this suppression of helix formation is only due to the introduction of attractive interactions and not due to the increase in repulsive interactions. One may infer this from the data of Fig.4a. There we show that increase in  $Z_0$  leads to larger repulsive forces which increases the propensity of helix formation.

The asymmetry in the distribution of charges along the polymer chain plays a crucial role in helix formation. In Fig.4e we show how helicity as measured by  $\langle H2 \rangle$  depends on the asymmetry parameter  $\psi$  for a constant value of  $Z_0$  which is set at  $Z_0 = 40$ s.u. For convenience, we now define a new asymmetry parameter  $\psi^*$  which depends on  $\psi$  as  $\psi^* = 1 - 2\psi$ . Note that  $\psi^* = +1$  implies that all the charges along the polymer chain are negative while  $\psi = -1$  denotes that all the charges are positive. If  $\psi^* = 0$  then there are statistically equal number of positive and negative charges in the polymer chain. Thus greater the value of  $|\psi^*|$  greater is the asymmetry in the distribution of charges.

We see that for  $\psi^* \sim 0$  helicity goes down, which indicates that when the strength of attractive interactions become comparable to the strength of repulsive interactions then helicity goes down. Thus helicity crucially relies on the presence of strong repulsive interactions which may arise from both positive and negative charges. This symmetry gives rise to the ‘U’ shape seen in Fig.4d.

In Fig.4a-c we examine the dependence of  $\langle H2 \rangle$  for a high value of asymmetry in the charge distribution ( $\psi = 0.1$  or  $\psi^* = 0.8$ ). We also establish that the trends observed in Fig.4 are robust even for lower asymmetry in charge distribution, i.e for  $\psi^* = 0.4$  (or  $\psi = 0.3$ ) albeit with a smaller value of  $\langle H2 \rangle$  as expected. This is shown in Fig.S1 of the Supplementary Information (SI).

Finally, we plot a state diagram using these parameters, using  $\kappa = 200k_B T/a^2$  (same as in Fig.1) to obtain the parameter space which is conducive to

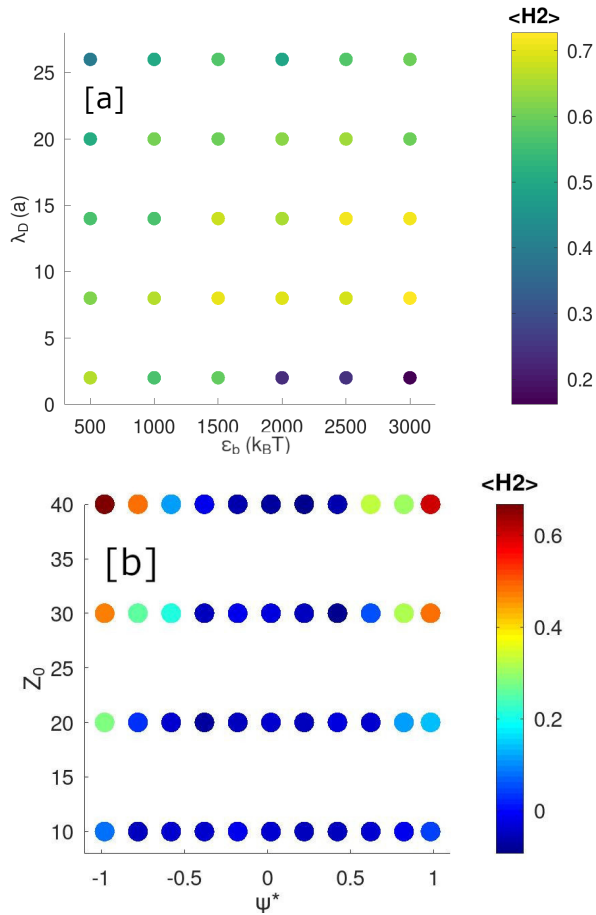


Figure 5. **State diagram of helix formation:** Figure shows the parameter space conducive to helix formation. In (a) we show the phase diagram with respect to the Debye length  $\lambda_d$  and the bending energy  $\epsilon_B$ . The maximum value of the charge in the polymer chain is  $Z_0 = 40$  s.u and the asymmetry parameter  $\psi = 0.1$  or  $\psi^* = 0.8$ . In (b) we show the phase diagram with respect to the charge  $Z_0$  and the asymmetry parameter  $\psi^*$  which is related to  $\psi$  as  $\psi^* = -2(\psi - 0.5)$ . We keep the Debye length  $\lambda_d = 5a$  and the bending energy  $\epsilon_B = 200k_B T$ . In both (a) and (b) we switch on charges at  $t = 10\tau$  and the average is computed over an interval of  $10\tau$ .

helix formation. In Fig.5a we show the state diagram with Debye length  $\lambda_D$  on the y-axis and the bending energy  $\epsilon_B$  on the x-axis. We keep  $Z_0$  and the charge distribution asymmetry parameter  $\psi$  the same as in Fig.1. We note that for  $\lambda_D < 6a$ ,  $\langle H2 \rangle$  shows a decrease with increase in  $\epsilon_B$  beyond  $1200k_B T$ . This indicates that for relatively more rigid chains the helix formation is suppressed as has already been shown in Fig.4b. However, for intermediate values of  $\lambda_D$  (i.e.  $\lambda_D \approx 10a$ ), this suppression in propensity to form helices is not observed. This is because each monomer interacts electrostatically with a larger number of monomers along the polymer chain. However, for higher values of  $\lambda_D$  ( $\lambda_D > 15a$ ), the propensity to form helices again decreases. This is consistent with the non-monotonic

behaviour of  $\langle H2 \rangle$  with increase in  $\lambda_D$  as established in Fig.4c and is for the same reason as explained. In Fig.5b we plot another state diagram keeping the  $\lambda_D$  and  $\epsilon_B$  fixed with the values being the same as that of Fig.1. Here we vary  $Z_0$  and  $\psi^*$  to plot the state diagram. We note that for small values of  $Z_0$ ,  $\langle H2 \rangle \approx 0$  while for higher values of  $Z_0$ , we obtain high values of  $\langle H2 \rangle$  only when  $\psi^* \approx \pm 1$ . These trends are consistent with those established in Fig.4a and Fig.4e. This once again emphasises that asymmetry in charge distribution of monomers along the chain is crucial to helix formation.

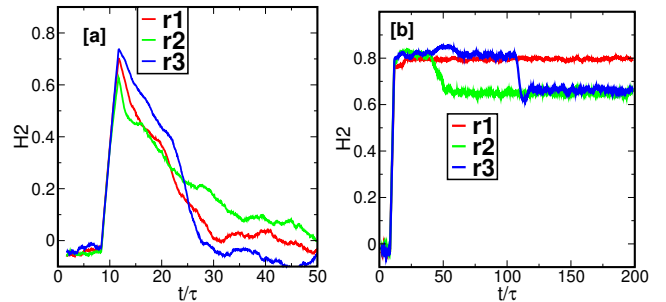


Figure 6. **Stabilization of transient helices:** To examine whether geometric confinement is able to stabilize the transient helices we induce helix formation in a cuboid. The length of the cuboidal box  $L_c = 1.1R_c$ , where  $R_c$  is the contour length of the polymer chain having 50 monomers. The width of the cuboid was  $W_c = 0.1R_c$ . We implement walls of the cuboid by WCA interactions and we keep the parameters identical to that in Fig.1. We switch on electrostatic interactions due to charges at  $10\tau$ . In (a) we show  $H2$  (running averaged over  $0.33\tau$ ) as a function of simulation time for an unconfined chain of 50 monomers for 3 independent runs. We see that the helix formed is transient and gradually dissolves with time. In (b) we show again a chain of 50 monomers similar to that of (a) but under confinement. We see that  $H2$  (running averaged over  $0.33\tau$ ) shows a high value even at long times for 3 independent runs. Thus geometric confinement lead to the stabilization of helices.

### C. Confinement stabilizes helices

We now study whether imposing geometric confinement leads to the emergence of long-lived helices in our model. To investigate this, we simulate the same system confined within a cuboid, where the rigid walls which are modelled by inducing repulsive WCA interactions to prevent the monomers crossing the walls, refer Fig.6. Thus we show that the transient helices formed due to electrostatic interactions between charged monomers may be stabilized or made long lived under confinement. In Fig.6a we show that  $H2$  or helicity for an unconfined chain dissolves away by  $50\tau$  whereas the helicity ( $H2$ ) for a (b) chain under confinement shows that  $H2$  fluctuates about a high value even at long times. Thus geometric confinement leads to stable helices due to electrostatic

interactions.

How does geometric confinement lead to the formation of stable helices? As mentioned before, the transient helices dissolve as the pitch of the helix increases and the polymer chain stretches out axially. This is due to the predominantly repulsive, electrostatic interactions between monomers and the bending energy cost due to semiflexibility. However, if the polymer is placed in a cuboidal box with length  $L_c = 1.1R_c$  ( $R_c$  is the initial contour length of the uncharged chain), the confinement prevents the stretching of the polymer chain axially and thus stops the unwinding process. This leads to the formation of long lived stable helices. Thus a geometric confinement with the axial dimension  $L_c \sim R_c$  successfully leads to long lived helical structures.

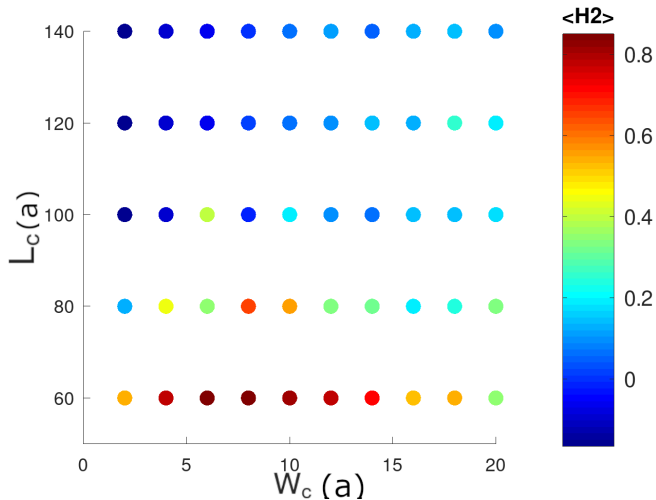


**Figure 7. Aspect ratios of cuboidal confinement conducive to helix formation:** To examine the ranges of  $W_c$  (width of the confining cuboid) and  $L_c$  (length of the confining cuboid) for which we obtain stable helix formation. We switch on electrostatic interactions due to charges at  $10\tau$  and measure  $\langle H2 \rangle$  over the next  $190\tau$ . The other parameters are identical to that of Fig1. The value of  $R_c$  is  $49a$  where  $a$  is the unit of length in our simulations.

This again leads to questions about the range of aspect ratios that are conducive to helix formation. To investigate this, we systematically vary the width  $W_c$  and length of the cuboid  $L_c$  of the cuboid with a square cross-section. We switch on charges at  $t = 10\tau$  and compute  $\langle H2 \rangle$  over the next  $190\tau$ . We plot a colour map showing the range of  $W_c$  and  $L_c$  conducive to stable helix formation, re-

fer Fig.7. We see that we obtain helix formation only when  $L_c \sim R_c$  and also requires intermediate values of  $W_c$ . When the values of  $W_c$  are small the monomers are unable to move significantly from the axis, thus leading to a suppression of helix formation. For large values of  $W_c$  the polymer may stretch out diagonally as a response to repulsive forces. Thus one may attain long-lived, helical structures due to electrostatic interactions between charged monomers in a polymer under confinement with the aspect ratio chosen suitably.

#### IV. DISCUSSIONS

Through this study, we have established a generic mechanism by which the helical motif may spontaneously emerge in several bio-molecules. We posit that such emergent structures may arise due to the induction of charges along the bio-polymer chain contour due to local changes in solvent conditions. However, these structures have to rely on other mechanisms to remain long-lived. Free-standing helices formed due to the switching on of screened Coulomb interactions are transient. In the presence of confinement, these helices become long-lived. In our study, we often use large Debye lengths ( $\approx 10a$ ). Such large values of the Debye length are unlikely to arise in natural polyelectrolytes. However, in this study we show that the mechanism of helix formation is robust even for such high values of the Debye lengths, which may be realized in experiments with highly deionized solvents.

The helices we observe in our simulations do not have a preferential handedness and may have an equal number of left-handed and right-handed segments. For most, bio-molecules however, there is a preferred handedness when the molecules attain helical conformations. Future investigations may shed light on this aspect and elucidate how a preferred handedness emerges. This will require incorporating specific constraints beyond the mechanism outlined here.

#### V. ACKNOWLEDGEMENTS

A.C., with DST-SERB identification SQUID-1973-AC-4067, acknowledges funding by DST-India, project MTR/2019/000078 and CRG/2021/007824. A.C also acknowledges discussions in meetings organized by ICTS, Bangalore.

[1] Nancy Kleckner, Jay K Fisher, Mathieu Stouf, Martin A White, David Bates, and Guillaume Witz. The bacterial nucleoid: nature, dynamics and sister segregation. *Current Opinion in Microbiology*, 22:127–137, 2014. Growth and development: eukaryotes/ prokaryotes.

[2] Roberto Dominguez and Kenneth C. Holmes. Actin structure and function. *Annual Review of Biophysics*, 40(1):169–186, June 2011.

[3] Matthew D. Shoulders and Ronald T. Raines. Collagen structure and stability. *Annual Review of Biochemistry*, 78(1):929–958, June 2009.

- [4] Jayanth R. Banavar, Trinh X. Hoang, Amos Maritan, Flavio Seno, and Antonio Trovato. Unified perspective on proteins: A physics approach. *Physical Review E*, 70(4), October 2004.
- [5] Jay K. Fisher, Aude Bourniquel, Guillaume Witz, Beth Weiner, Mara Prentiss, and Nancy Kleckner. Four-dimensional imaging of e. coli nucleoid organization and dynamics in living cells. *Cell*, 153(4):882–895, May 2013.
- [6] Amos Maritan, Cristian Micheletti, Antonio Trovato, and Jayanth R. Banavar. Optimal shapes of compact strings. *Nature*, 406(6793):287–290, July 2000.
- [7] B. Pokroy, S. H. Kang, L. Mahadevan, and J. Aizenberg. Self-organization of a mesoscale bristle into ordered, hierarchical helical assemblies. *Science*, 323(5911):237–240, January 2009.
- [8] Sid Ahmed Sabeur, Fatima Hamdache, and Friederike Schmid. Kinetically driven helix formation during the homopolymer collapse process. *Physical Review E*, 77(2), February 2008.
- [9] Huaping Li and Alkan Kabakçioğlu. Role of helicity in DNA hairpin folding dynamics. *Physical Review Letters*, 121(13), September 2018.
- [10] Daniel A. Vega, Andrey Milchev, Friederike Schmid, and Mariano Febbo. Anomalous slowdown of polymer detachment dynamics on carbon nanotubes. *Physical Review Letters*, 122(21), May 2019.
- [11] Y. Snir. Entropically driven helix formation. *Science*, 307(5712):1067–1067, February 2005.
- [12] S. J. Gerbode, J. R. Puzey, A. G. McCormick, and L. Mahadevan. How the cucumber tendril coils and overwinds. *Science*, 337(6098):1087–1091, August 2012.
- [13] Y. Forterre and J. Dumais. Generating helices in nature. *Science*, 333(6050):1715–1716, September 2011.
- [14] Bipul Biswas, Debarshi Mitra, Fayis KP, Suresh Bhat, Apratim Chatterji, and Guruswamy Kumaraswamy. Rigidity dictates spontaneous helix formation of thermoresponsive colloidal chains in poor solvent. *ACS Nano*, 15(12):19702–19711, December 2021.
- [15] Debasish Chaudhuri and Bela M. Mulder. Spontaneous helicity of a polymer with side loops confined to a cylinder. *Physical Review Letters*, 108(26), June 2012.
- [16] S. Srivastava, A. Santos, K. Critchley, K.-S. Kim, P. Podsiadlo, K. Sun, J. Lee, C. Xu, G. D. Lilly, S. C. Glotzer, and N. A. Kotov. Light-controlled self-assembly of semiconductor nanoparticles into twisted ribbons. *Science*, 327(5971):1355–1359, February 2010.
- [17] Tamaki Nakano and Yoshio Okamoto. Synthetic helical polymers: conformation and function. *Chemical Reviews*, 101(12):4013–4038, November 2001.
- [18] Sheng Zhong, Honggang Cui, Zhiyun Chen, Karen L. Wooley, and Darrin J. Pochan. Helix self-assembly through the coiling of cylindrical micelles. *Soft Matter*, 4(1):90–93, 2008.
- [19] Lingxiang Jiang, Julius W. J. de Folter, Jianbin Huang, Albert P. Philipse, Willem K. Kegels, and Andrei V. Petukhov. Helical colloidal sphere structures through thermo-reversible co-assembly with molecular microtubes. *Angewandte Chemie*, 125(12):3448–3452, February 2013.
- [20] G. Singh, H. Chan, A. Baskin, E. Gelman, N. Repnin, P. Kral, and R. Klajn. Self-assembly of magnetite nanocubes into helical superstructures. *Science*, 345(6201):1149–1153, July 2014.
- [21] Q. Guo, A. K. Mehta, M. A. Grover, W. Chen, D. G. Lynn, and Z. Chen. Shape selection and multi-stability in helical ribbons. *Applied Physics Letters*, 104(21):211901, May 2014.
- [22] Yunlong Zhou, Ryan L. Marson, Greg van Anders, Jian Zhu, Guanxiang Ma, Peter Ercius, Kai Sun, Bongjun Yeom, Sharon C. Glotzer, and Nicholas A. Kotov. Biomimetic hierarchical assembly of helical supraparticles from chiral nanoparticles. *ACS Nano*, 10(3):3248–3256, March 2016.
- [23] Xiang Yang Kong and Zhong Lin Wang. Spontaneous polarization-induced nanohelices, nanosprings, and nanorings of piezoelectric nanobelts. *Nano Letters*, 3(12):1625–1631, December 2003.
- [24] Kevin Stratford, Oliver Henrich, Juho S Lintuvuori, ME Cates, and Davide Marenduzzo. Self-assembly of colloid-cholesteric composites provides a possible route to switchable optical materials. *Nature communications*, 5(1):1–8, 2014.
- [25] Qun li Lei, Ran Ni, and Yu qiang Ma. Self-assembled chiral photonic crystals from a colloidal helix racemate. *ACS Nano*, 12(7):6860–6870, June 2018.
- [26] Wenchun Feng, Ji-Young Kim, Xinzhi Wang, Heather A Calcaterra, Zhibei Qu, Louisa Meshi, and Nicholas A Kotov. Assembly of mesoscale helices with near-unity enantiomeric excess and light-matter interactions for chiral semiconductors. *Science Advances*, 3(3):e1601159, 2017.
- [27] Yong Wang, Jun Xu, Yawen Wang, and Hongyu Chen. Emerging chirality in nanoscience. *Chem. Soc. Rev.*, 42(7):2930–2962, 2013.
- [28] W. Wang, K. Yang, J. Gaillard, P.R. Bandaru, and A. M. Rao. Rational synthesis of helically coiled carbon nanowires and nanotubes through the use of tin and indium catalysts. *Advanced Materials*, 20(1):179–182, January 2008.
- [29] Hai-Feng Zhang, Chong-Min Wang, and Lai-Sheng Wang. Helical crystalline SiC/SiO<sub>2</sub>core-shell nanowires. *Nano Letters*, 2(9):941–944, September 2002.
- [30] Hai-Feng Zhang, Chong-Min Wang, Edgar C. Buck, and Lai-Sheng Wang. Synthesis, characterization, and manipulation of helical SiO<sub>2</sub>nanosprings. *Nano Letters*, 3(5):577–580, May 2003.
- [31] Lichun Liu, Sang-Hoon Yoo, Sang A. Lee, and Sungho Park. Wet-chemical synthesis of palladium nanosprings. *Nano Letters*, 11(9):3979–3982, September 2011.
- [32] D. C. Rapaport. Molecular dynamics simulation of polymer helix formation using rigid-link methods. *Physical Review E*, 66(1), July 2002.
- [33] Tatjana Škrbić, Jayanth R. Banavar, and Achille Giacometti. Chain stiffness bridges conventional polymer and bio-molecular phases. *The Journal of Chemical Physics*, 151(17):174901, November 2019.
- [34] Debarshi Mitra and Apratim Chatterji. Transient helix formation in charged semiflexible polymers without confinement effects. *Journal of Physics: Condensed Matter*, 33(4):044001, October 2020.
- [35] Bipul Biswas, Raj Kumar Manna, Abhrajit Laskar, P. B. Sunil Kumar, Ronojoy Adhikari, and Guruswamy Kumaraswamy. Linking catalyst-coated isotropic colloids into “active” flexible chains enhances their diffusivity. *ACS Nano*, 11(10):10025–10031, September 2017.
- [36] Andrey V. Dobrynin. Electrostatic persistence length of semiflexible and flexible polyelectrolytes. *Macromolecules*, 38(22):9304–9314, October 2005.